

Discounted Mean-Field Game model of a dense static crowd with variable information crossed by an intruder

Matteo Butano ^{1*}, Cécile Appert-Rolland ², Denis Ullmo ¹

¹ Université Paris-Saclay, CNRS, LPTMS, 91405, Orsay, France

² Université Paris-Saclay, CNRS, IJCLab, 91405, Orsay, France

* matteo.butano@universite-paris-saclay.fr

February 20, 2023

Abstract

It has been proven that the displayed anticipation pattern of a dense crowd crossed by an intruder can be successfully described by a minimal Mean-Field Games model. However, experiments show that when pedestrians have limited knowledge, the global anticipation dynamics becomes less optimal. Here we reproduce this with the same MFG model, with the addition of only one parameter, a discount factor γ that tells the time scale of agents' anticipation. We present a comparison between the discounted MFG and the experimental data, also providing new analytic results and important insight about how the introduction of γ modifies the model.

Contents

1	Introduction	2
2	The Mean-Field Games model	4
2.1	The discounted equations	4
2.2	Discounted ergodic state	6
2.3	Passing to the moving frame	7
3	Comparisons with experiment	7
3.1	Pedestrians facing the obstacle	8
3.2	Pedestrians randomly oriented	8
3.3	Pedestrians giving their back to the obstacle	10
4	Conclusion	10
A	Alternative formulation of MFG	13
B	Details on the ergodic problem	14
C	Details on the numerics	15
	References	15

1 Introduction

As discussed by Hoogendorn et al. [1], pedestrian motion is a multi-scale endeavour that needs to be described at different levels, and one typically distinguishes the strategic level (what are the goals of the travel and the general timing), the tactical level (which route to take) and the operational level (how to move on that route). If the strategic and tactical levels naturally assume some form of long term optimisation, it is on the other hand quite generally expected that the operational level, especially for dense crowds, could be described by dynamical models involving physical and social forces [2], and possibly a short term (up to the next collision) anticipation [3–5]. However, the comparison of experimental data from a control experiment involving a static dense crowd [6] with various simulation models showed that [7], in such cases, it appears necessary to include long term anticipation in order to reproduce the observed experimental features. This could be achieved with a very simple Mean-Field Game model. Mean-Field Games, introduced by Lasry and Lions [8, 9] as well as Huang et al. [10] is a mathematical formalism in which both anticipation and competitive optimization between the agents, here pedestrians, are accounted for at the mean field level. The fact that it may provide a good description of human behaviour is a priori non trivial for at least two reasons. The first one is that the agents clearly cannot compute the predictions of the Mean-Field Games model, the second is that they usually do not have the perfect information assumed in the model.

The answer to this first concern is, as in many game theoretical context, that we expect the behaviour of the agents to be learnt rather than computed. In the same way that we do not need to use the laws of dynamics to know where a ball thrown in the air will land, there are in daily life many circumstances which are familiar enough that we can, by instinct, predict the behavior of the crowd and act accordingly. It is clearly in these circumstances that we can expect a Mean-Field-Game description to apply, and this was the case in the experimental context of [6]. The second of these concerns, which will be the main focus of this paper, was actually addressed experimentally in [6]. The experimental setup studied there consisted in the crossing of a dense static crowd by a cylindrical intruder. However, the experiments have been performed in three configurations: with pedestrian facing the obstacle, being randomly oriented, or giving their back to it. Moreover, in the latter case pedestrians were asked not to anticipate, while no such instruction was given in the first two cases. Clearly, if, in this simple context, we can expect the first configuration to give participants perfect information about the system, this is not the case for the other two, and indeed, as seen on Fig. 1, the observed density maps and velocity fields, obtained by an average over repeated realizations of the experiment, clearly differ significantly in the three cases. In [7], we focused only on the case where pedestrians were facing the obstacle (for an average density of $2.5 \text{ ped}/\text{m}^2$, slightly lower than the one shown in Fig. 1(a), but displaying the same features). Observing Figure 1(a), we see that in the frontal configuration, individuals move in advance, temporarily accepting a higher local density in order to get rid of the obstacle sooner, showing evidence of a trade-off dynamics. The crowd's density increases on the sides and depletes in front of and behind the cylinder, with pedestrians moving outward to avoid its arrival and inward to regain a less congested position, always perpendicularly to the obstacle's motion. This clearly is an anticipatory dynamics, that, most importantly, does not solely depend on the distance from

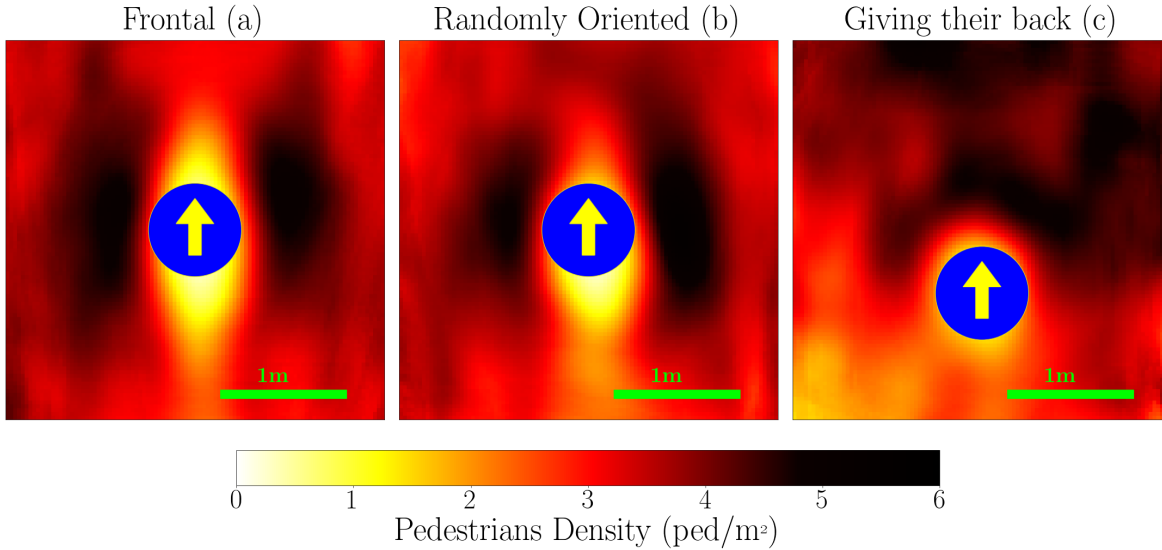


Figure 1: Experimental results of the passage of a cylindrical intruder through a static dense crowd for an average density of $\sim 3.5 \text{ ped/m}^2$ for three different configurations. In (a) pedestrians were all facing the obstacle, in (b) they were randomly oriented and in (c) participants were asked to give their back to it. Data from [6].

the obstacle, meaning that even pedestrians far from it know that it will arrive and, depending on its speed, they will start moving accordingly. However, when individuals are placed randomly, as in the second panel of Figure 1, we notice a shorter corridor of anticipation in front of the obstacles, but with similar accumulation patterns on its sides. When pedestrians in the experiment were asked not to anticipate and to give their back to the incoming intruder, effectively looking away from it, as the third panels of Figure 1 shows, we observe that the accumulation of the individuals moves from the sides to the front of the obstacle, similarly to what happens in analog configurations with granular matter [7].

The main goal of this paper is to demonstrate that at least in the experimental setup corresponding to Fig.1, this lack of information can be taken into account simply by introducing a *discount factor*, i.e. a term discounting the cost of actions in a future further than a certain cut-off, to the model already used in [7] to simulate the frontal case. Such discount factors are, for example, usually introduced in optimization problem spanning a long time period (typically in economic context) to express the unwillingness of agents to wait too long for a reward. Here however we use it as a way to simulate the shortsightedness of pedestrians. We shall in section 2 introduce the corresponding Mean-Field-Game model and give some discussion about its generic behavior. Then, section 3 will feature the comparison with the three experimental cases discussed above. We will first come back on the case where pedestrians were facing the obstacle, providing more details about the results presented in [7]. Then, the remnant experimental setups will be considered, and we will show how the introduction of the discount factor helps in modeling these configurations.

2 The Mean-Field Games model

Mean-Field Games (MFG) constitutes a relatively new field of research. Its foundations are in the works of J.-M. Lasry and P.-L. Lions [8, 9], and of M. Huang, R. P. Malhamé and P. E. Caines [10]. During the years, many works have been focused on the mathematical properties of MFG [11–15]. Although there are applications of MFG to pedestrian dynamics [16], to the best of our knowledge comparisons of crowds simulated with MFG to experimental data [7] are rare. A general and mathematically rigorous discussion of the foundations of MFG being found in the book [14], a physicist-friendly version being exposed in [17], here we will limit ourselves to essentials.

2.1 The discounted equations

In the specific settings of our MFG model, each agent's *state variable* $\vec{X}(t) \in \mathbb{R}^2$, representing their position, evolves following the *Langevin equation*

$$\dot{\vec{X}} = \vec{a}(t) + \sigma \vec{\xi}(t), \quad (1)$$

where $\vec{\xi}(t)$ is a two dimensional Gaussian white noise, and \vec{a} is the drift velocity, the *control parameter* that represents the strategy players choose by minimizing the discounted cost functional defined, in this case, as

$$c[\vec{a}](\vec{x}, t) = \mathbb{E} \left\{ \int_t^T \mathcal{L}(\vec{x}, \tau)[m] e^{\gamma(t-\tau)} d\tau + e^{\gamma(t-T)} c_T(\vec{x}_T) \right\} \quad (2)$$

where c_T is a *terminal cost*, that could be used to represent a target for pedestrians, e.g. an exit, γ is the discount factor, that tells how far into the future agents will look while optimizing, and

$$\mathcal{L}(\vec{x}, \tau)[m] = \frac{\mu}{2} (\vec{a}(\tau))^2 - V[m](\vec{x}, \tau) \quad (3)$$

can be seen as the term describing the agents' preferences. In fact, the squared velocity tells that going too fast is detrimental, and that the best would be to stand still, but the presence of the external world, represented by the potential term

$$V[m](\vec{x}, t) = gm(\vec{x}, t) + U_0(\vec{x}, t), \quad (4)$$

describing the interaction with the others and with the environment, cause agents to actually move. Here the environment would be the moving cylinder, but different scenarios could be accounted for. The main assumptions of MFG are that all agents are equal and the interaction with others is of mean-field type, determined only through the average density

$$m(\vec{x}, t) = \lim_{N \rightarrow +\infty} \mathbb{E} \left[\frac{1}{N} \sum_{i=1}^N \delta(\vec{x} - \vec{X}_i(t)) \right],$$

On the other hand, the term $U_0(\vec{x}, t)$ describes the interaction with the environment, and it is what is used to describe the scenario we simulate our MFG pedestrians in. The quantity of interest is then the *value function*

$$u(\vec{x}, t) = \inf_{\vec{a}} c[\vec{a}](\vec{x}, t). \quad (5)$$

At this point, we see that we can write

$$\begin{aligned} u(\vec{x}, t) &= \inf_{\vec{a}} \mathbb{E} \left\{ \int_t^T \mathcal{L}(\vec{x}, \tau) [m] e^{\gamma(t-\tau)} d\tau + e^{\gamma(t-T)} c_T(\vec{x}_T) \right\} \\ &= \inf_{\vec{a}} \mathbb{E} \left\{ \int_t^{t+dt} \mathcal{L}(\vec{x}, \tau) [m] e^{\gamma(t-\tau)} d\tau + e^{-\gamma dt} \left(\int_{t+dt}^T \mathcal{L}(\vec{x}, \tau) [m] e^{\gamma(t+dt-\tau)} d\tau + e^{\gamma(t+dt-T)} c_T(\vec{x}_T) \right) \right\} \end{aligned}$$

that, by making use of the *dynamic programming principle* [18] can be written as

$$\begin{aligned} u(\vec{x}, t) &= \inf_{\vec{a}} \left[\mathcal{L}(\vec{x}, t) dt + e^{-\gamma dt} u(\vec{x} + \vec{a} dt, t + dt) \right] \\ &= \inf_{\vec{a}} \left[\mathcal{L}(\vec{x}, t) dt + e^{-\gamma dt} \left(u(\vec{x}, t) + \frac{d}{dt} u(\vec{x}, t) dt \right) \right] \\ &\stackrel{\text{Ito}}{=} \inf_{\vec{a}} \left\{ \mathcal{L}(\vec{x}, t) dt + (1 - \gamma dt) \left[u(\vec{x}, t) + dt \left(\partial_t u + \vec{a} \cdot \vec{\nabla} u + \frac{\sigma^2}{2} \Delta u \right) \right] \right\} \end{aligned}$$

where in the last passage the Ito chain rule has been used to calculate the total time derivative of the value function. Then, by keeping only terms at first order in dt what is left is

$$u = u + dt \left(\partial_t u - V[m] + \frac{\sigma^2}{2} \Delta u + \gamma u + \inf_{\vec{a}} \left\{ \frac{\mu}{2} \vec{a}^2 + \vec{a} \cdot \vec{\nabla} u \right\} \right),$$

which, simplifying dt and u , becomes

$$0 = \partial_t u - V[m] + \frac{\sigma^2}{2} \Delta u - \gamma u + \inf_{\vec{a}} \left\{ \frac{\mu}{2} \vec{a}^2 + \vec{a} \cdot \vec{\nabla} u \right\}. \quad (6)$$

At this point, by minimizing the term in the curly brackets with respect to \vec{a} we find that the optimal velocity is given by

$$\vec{a}^* = -\frac{\vec{\nabla} u}{\mu}. \quad (7)$$

Finally, when (7) is plugged back in (6), we find that the value function solves the following *Hamilton-Jacobi-Bellman* equation

$$\begin{cases} \partial_t u = -\frac{\sigma^2}{2} \Delta u + \frac{1}{2\mu} (\vec{\nabla} u)^2 + \gamma u + V[m] \\ u(\vec{x}, t = T) = c_T(\vec{x}) \end{cases} \quad (8)$$

This is a backward equation, that is solved starting from the terminal condition expressed by the terminal cost $c_T(\vec{x})$, which is useful to set goals to be reached by time T by the agents, e.g. exiting a room or reaching a certain area. Then, given the stochastic evolution of each player's state variable, we know that the corresponding density evolves following the Kolmogorov-Fokker-Plank equation

$$\begin{cases} \partial_t m = \frac{\sigma^2}{2} \Delta m + \frac{1}{\mu} \nabla \cdot (m \nabla u) \\ m(\vec{x}, t = 0) = m_0(\vec{x}) \end{cases} \quad (9)$$

a forward equation solved starting from an initial density profile. It should be observed that it is possible to cast the problem in a different formulation using a Cole-Hopf transformation, something extensively debated in [7, 17], although in the case of $\gamma = 0$. We dedicate the appendix A to show how this formulation evolves for a general γ .

2.2 Discounted ergodic state

In the case of no explicit time dependence in the cost functional (2), for times sufficiently larger than the initial time and smaller than T it has been shown, for example in [8], that for a generic MFG model a *stationary* or *ergodic state* exists, where the density becomes time independent $m(\vec{x}, t) \simeq m^e(\vec{x})$ and the value function decouples its time and spatial dependence, so that we can write

$$u(\vec{x}, t) \simeq u^e(\vec{x}) + f(t). \quad (10)$$

For the non discounted problem, meaning $\gamma = 0$, such an ergodic state has been extensively studied, see [19], and it has been shown that $f_{\gamma=0}(t) = -\lambda t$, where λ is a constant whose value is determined at the end of Appendix B. The scope of this section is to study the ergodic state of a MFG for a generic γ . The reason we do so is that the experimental data shown in Figure 1 focus on the passage of the cylinder through the crowd at an intermediate time, when the intruder was surrounded by a sufficiently high number of pedestrians both in front and behind, to make the measurement more meaningful. Experimenters did not focus on what happens when the cylinder enters or leave the crowded space. We then claim that the experimental data can be reproduced by the ergodic regime of our Mean-Field Game. Our hypothesis is that, in the case of $\gamma > 0$ (10) is still valid, thus, by plugging it in (8), we obtain

$$\frac{\sigma^2}{2} \Delta u^e - \frac{1}{2\mu} (\vec{\nabla} u^e)^2 + f'(t) - \gamma(u^e(\vec{x}) + f(t)) = V[m], \quad (11)$$

then, in order to get rid of any explicit time dependence in the equation, and therefore in $u^e(\vec{x})$, we impose that $f'(t) = \gamma f(t) - \lambda$, which gives $f(t) = ke^{\gamma t} + \frac{\lambda}{\gamma}$, that we plug back in (10) to obtain that, for intermediate times, the ergodic state of the value function is

$$u(\vec{x}, t) \simeq u^e(\vec{x}) + ke^{\gamma t} + \frac{\lambda}{\gamma}.$$

In order to fix k , we turn our attention to the behavior of the ergodic state for small values of the discount factor, i.e. when $\gamma \rightarrow +\infty$. In this case we can write

$$u(\vec{x}, t) \simeq u^e(\vec{x}) + k + k\gamma t + \frac{\lambda}{\gamma}.$$

By taking $k = -\lambda/\gamma$ one recovers $f_{\gamma=0}(t) = -\lambda t$. The ergodic state of the value function for the discounted MFG is therefore

$$u(x, t) \simeq u^e(x) + \frac{\lambda}{\gamma}(1 - e^{\gamma t}), \quad t_0 \ll t \ll T. \quad (12)$$

The equations followed by the position dependent part of the ergodic state both for the density and the value function for a general MFG model with a potential V not explicitly depending on time are then

$$\frac{\sigma^2}{2} \Delta u^e - \frac{1}{2\mu} (\vec{\nabla} u^e)^2 - \gamma u^e(x) - \lambda - V[m^e] = 0, \quad (13)$$

$$\frac{\sigma^2}{2} \Delta m^e + \frac{1}{\mu} \nabla \cdot (m^e \nabla u^e) = 0. \quad (14)$$

2.3 Passing to the moving frame

When we introduced the ergodic state in subsection 2.2 we mentioned the necessity of the absence of any explicit time dependence in the cost functional (2) for equations (13) and (14) to be possible. This clashes with the fact that we simulate the presence of the intruder by using a cylindrical potential whose position evolves with time. In order to overcome this inconvenient, we change the reference frame in which we describe the experimental setting by passing from the point of view of the laboratory to the point of view of the cylinder, by defining the following quantities

$$\tilde{u}(\vec{x} - \vec{s}t, t) = u(\vec{x}, t), \quad \tilde{m}(\vec{x} - \vec{s}t, t) = m(\vec{x}, t).$$

In framework of the cylinder the potential becomes $\tilde{V}[\tilde{m}] = g\tilde{m} + \tilde{U}_0(\vec{x})$, not depending explicitly on time anymore, with

$$\tilde{U}_0(\vec{x}) = \begin{cases} +\infty & x < R \\ 0 & \text{otherwise} \end{cases} \quad (15)$$

where R is the radius of the cylinder. For all other quantities we observe that, in general,

$$\partial_t f(\vec{x}, t) = \frac{d}{dt} f(\vec{x}, t) = \frac{d}{dt} \tilde{f}(\vec{x} - \vec{s}t, t) = \partial_t \tilde{f} - \vec{s} \cdot \vec{\nabla} \tilde{f}. \quad (16)$$

where the total derivative is taken in the lab's reference frame. Then, using (16) in (8) and (9) gives us the time dependent version of the MFG equation in u and m variables in the moving frame

$$\partial_t \tilde{u} - \vec{s} \cdot \vec{\nabla} \tilde{u} = -\frac{\sigma^2}{2} \Delta \tilde{u} + \frac{1}{2\mu} (\vec{\nabla} \tilde{u})^2 + \gamma \tilde{u} + \tilde{V}[\tilde{m}] \quad (17)$$

$$\partial_t \tilde{m} - \vec{s} \cdot \vec{\nabla} \tilde{m} = \frac{\sigma^2}{2} \Delta \tilde{m} + \frac{1}{\mu} \nabla \cdot (\tilde{m} \nabla \tilde{u}) \quad (18)$$

whereas the corresponding equations for the ergodic state are

$$\frac{\sigma^2}{2} \Delta \tilde{u}^e - \frac{1}{2\mu} (\vec{\nabla} \tilde{u}^e)^2 - \vec{s} \cdot \vec{\nabla} \tilde{u}^e - \gamma \tilde{u}^e(x) - \lambda - \tilde{V}[\tilde{m}^e] = 0, \quad (19)$$

$$\frac{\sigma^2}{2} \Delta \tilde{m}^e + \frac{1}{\mu} \nabla \cdot (\tilde{m}^e \nabla \tilde{u}^e) + \vec{s} \cdot \vec{\nabla} \tilde{m}^e = 0. \quad (20)$$

As we said, we will compare to the experimental data showed in Figure 1 the stationary regime of the MFG density, i.e. the solution of (20), as was done in [7] where there was no discount factor, with details provided in Appendix B. However, it turns out that, when $\gamma > 0$, numerically solving (20), and thus (19), is more complicated than directly solving the MFG system given by (8) and (9) for each time between t_0 and T and then accessing the ergodic state by taking a snapshot of the density at an intermediate time $t_0 \ll t \ll T$. This is therefore what has been done here, with details provided in Appendix C.

3 Comparisons with experiment

At this point we have concluded the theoretical presentation of the Mean-Field Games model we plan to use to simulate the experimental settings previously discussed. We will deal with the

three different experimental configurations showed in Figure 1 separately. First, we will simulate the case, already studied in [7], where pedestrians were facing the obstacle, then, the case for pedestrians being randomly oriented is treated. Finally, we will deal with the case of pedestrians giving their back to the intruder and not anticipating.

Main Scales Our model contains many parameters, the tuning of which might be tedious and inefficient. Luckily, two main quantities can be defined as

$$\xi = \sqrt{\left| \frac{\mu \sigma^4}{2g m_0} \right|}, \quad c_s = \sqrt{\left| \frac{g m_0}{2\mu} \right|}$$

that are called, respectively, the *healing length*, a length scale and the *sound velocity*, a velocity scale. We understand them by imagining that the cylinder had an infinitely small radius and zero speed, so that we could consider it a punctual perturbation in an homogeneous density. The healing length would then be the distance up to which the density would deform, and the sound velocity the speed with which the density would return to its initial unperturbed state were the perturbation removed. Most importantly, it is the ratio between these scales and their counterparts for the cylinder, respectively its radius R and its speed s , that uniquely determine the MFG solution, as shown in [7]. Finally, another important scale of the problem is $1/\gamma$, the time scale over which the anticipation is performed. A large value of γ means that agents optimize only for the present, whereas a small γ means that agents can see further in the future and therefore anticipate more effectively.

3.1 Pedestrians facing the obstacle

In [7] we studied the case where pedestrians were facing the arriving cylinder. Under these circumstances, people could efficiently estimate the cylinder's size and velocity, thus the time it would take for the obstacle to reach them. We model such scenario by taking $\gamma = 0$, and the simulation is shown on the left column of Figure 2. Here we see how striking the resemblance to the experiment is. Starting from the density plot, we clearly see the vertically symmetric distribution of pedestrians, with a depletion prior and posterior to the obstacle passage and with an increase on the sides. Moreover, the velocity field obtained from the MFG model correctly display the lateral motion of pedestrians stepping aside to make room for the intruder. We believe MFG good performances should be attributed to an element that, as already discussed in [7], many pedestrian dynamics models, such as granular and social force models, struggle accounting for. This is the long term anticipatory behavior of individuals clearly captured in the experiment and naturally present in the very structure of MFG, namely by means of the backward-solved HJB equation (8). The back-propagation of information allows MFG agents to optimally anticipate the obstacle's arrival, and most notably without prescribing an anticipation time, contrarily to many models for crowds motion. Indeed, solving the MFG equations gives the Nash equilibrium velocity an agent should adopt for any given point in the simulated space, i.e. the strategy of motion which, in the spirit of (2), is best suited to avoid the obstacle and high density areas.

3.2 Pedestrians randomly oriented

In experimental configuration where participants were asked to orient themselves randomly we see, from the right column of Figure 3, that the main difference with the frontal case is in the decrease of the depletion in front of the obstacle, meaning that participants anticipate less. We

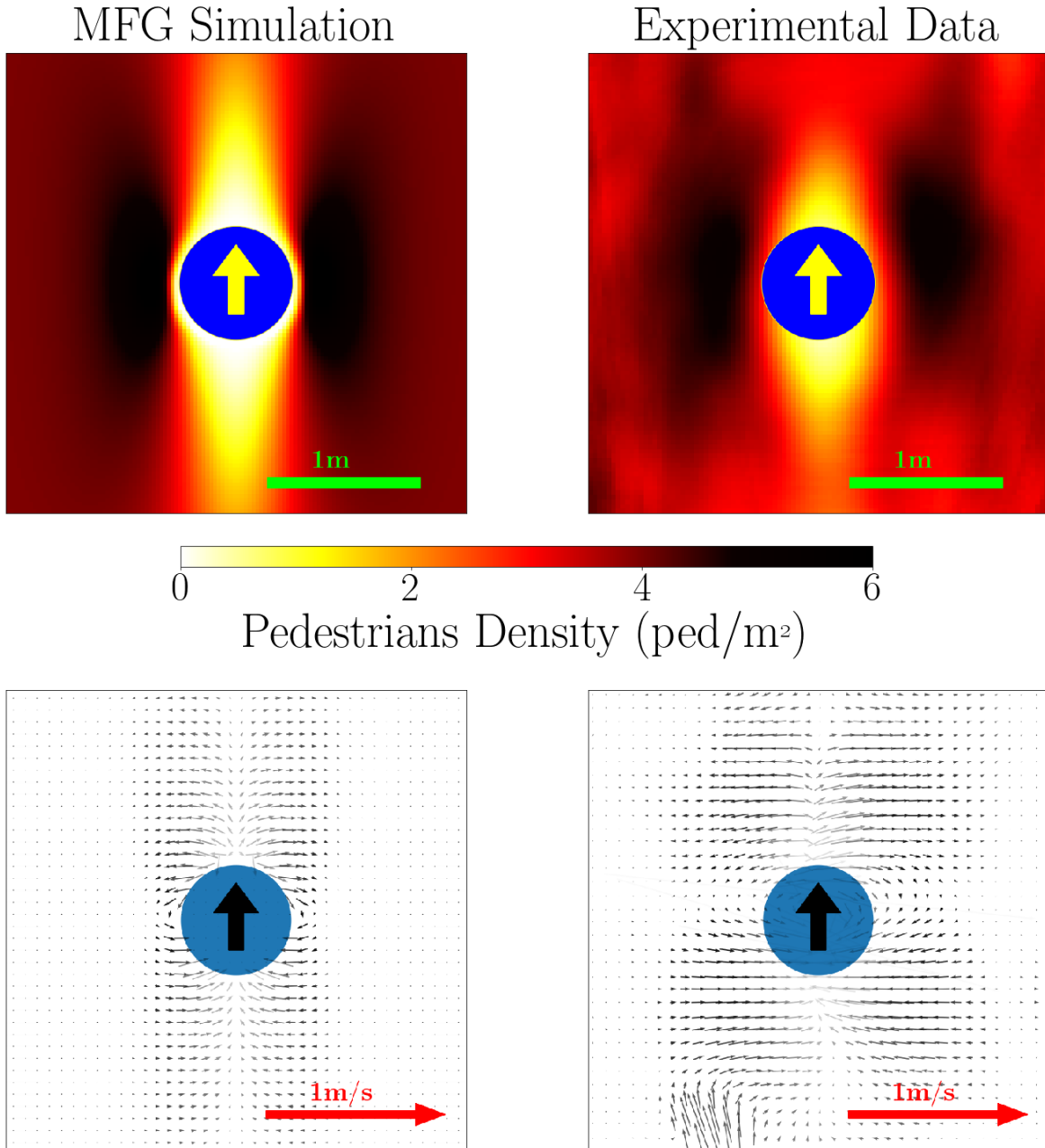


Figure 2: Qualitative comparison between density, first row, and velocity plots, second row, between the experiment, right column, and the ergodic state of the MFG model, with parameters $\xi = 0.2$, $c_s = 0.1$ and $\gamma = 0$, left column, for the case where all pedestrians were facing the incoming intruder.

can imagine that, when participants were placed randomly, only some of them could gather information about the obstacle visually, whereas the rest had to resort to all their other senses to decide how to react. This impacts the global anticipatory behavior and causes a later reaction to the obstacle arrival. The inclusion of the discount factor γ in our MFG is enough to describe the change in the crowd's avoidance strategy. The left column of Figure 3 shows the numerical solution of the MFG system for ξ and c_s as for the frontal case and with $\gamma = 0.5$. We can indeed observe that turning on the discount factor produces the desired effects, by reducing the crowd's displacement in front of the obstacle but still conserving the accumulation on the sides and the density depletion after its passage. Moreover, the simulated velocity field shows an increase in escaping dynamics in front of the cylinder and slight circulation around it.

3.3 Pedestrians giving their back to the obstacle

Finally, when participants in the experiment had to give their back to the obstacle and were asked not to anticipate, the observed behavior changed decisively. As the right panel of Figure 4 shows, having lost the visual information, it was harder to estimate the obstacle's velocity and direction of motion, resulting in pedestrians being pushed along by the intruder, behaving like granular material [7]. Behind the cylinder, on the other hand, no significant depletion is shown, and this we believe it is due to the diffusivity of the crowd, given the pedestrians' intention to have as much space as possible. The left column of Figure 4 shows the MFG simulation for $\xi = 0.4$, $c_s = 0.2$ and $\gamma = 6$. Here we recover the accumulation in front of the obstacle and the smaller depletion behind it. By looking at the velocity plots we clearly see that pedestrians in front of the cylinder are pushed by the intruder along the direction of its motion. Then, we also remark the agreement with the rotational motion around the obstacle, analogously to what would happen for granular inert matter, under purely mechanical forces. Again, as in the random case, we managed to recover the experimental behavior only by means of the discount factor. In fact, even though we have slightly modified ξ and c_s , to better fit the data, the solution still remains in the same quadrant of the MFG phase space described in [7]. This means that the discounting term correctly reproduces losses in anticipatory abilities.

4 Conclusion

In the present work we have provided a detailed description of the Mean-Field Games model used in [7] with the addition of a term discounting agents anticipation. Moreover, we have shown that such term helps modulating the simulated anticipatory behavior, making it possible to reproduce a wider range of crowd dynamic scenarios, as the comparison with the different experimental configurations has shown. This is all the more remarkable since we used the most simple and first ever proposed Mean-Field Game model [8], to which we just added a parameter, the discount factor. We strongly believe in the validity of our approach, not because we think people solve a coupled system of non-linear differential equations while walking, but because we believe humans have nevertheless, at least in simple cases, internalized some basic anticipation mechanisms that allow them to rapidly coordinate with the others and efficiently avoid eventual obstacles.

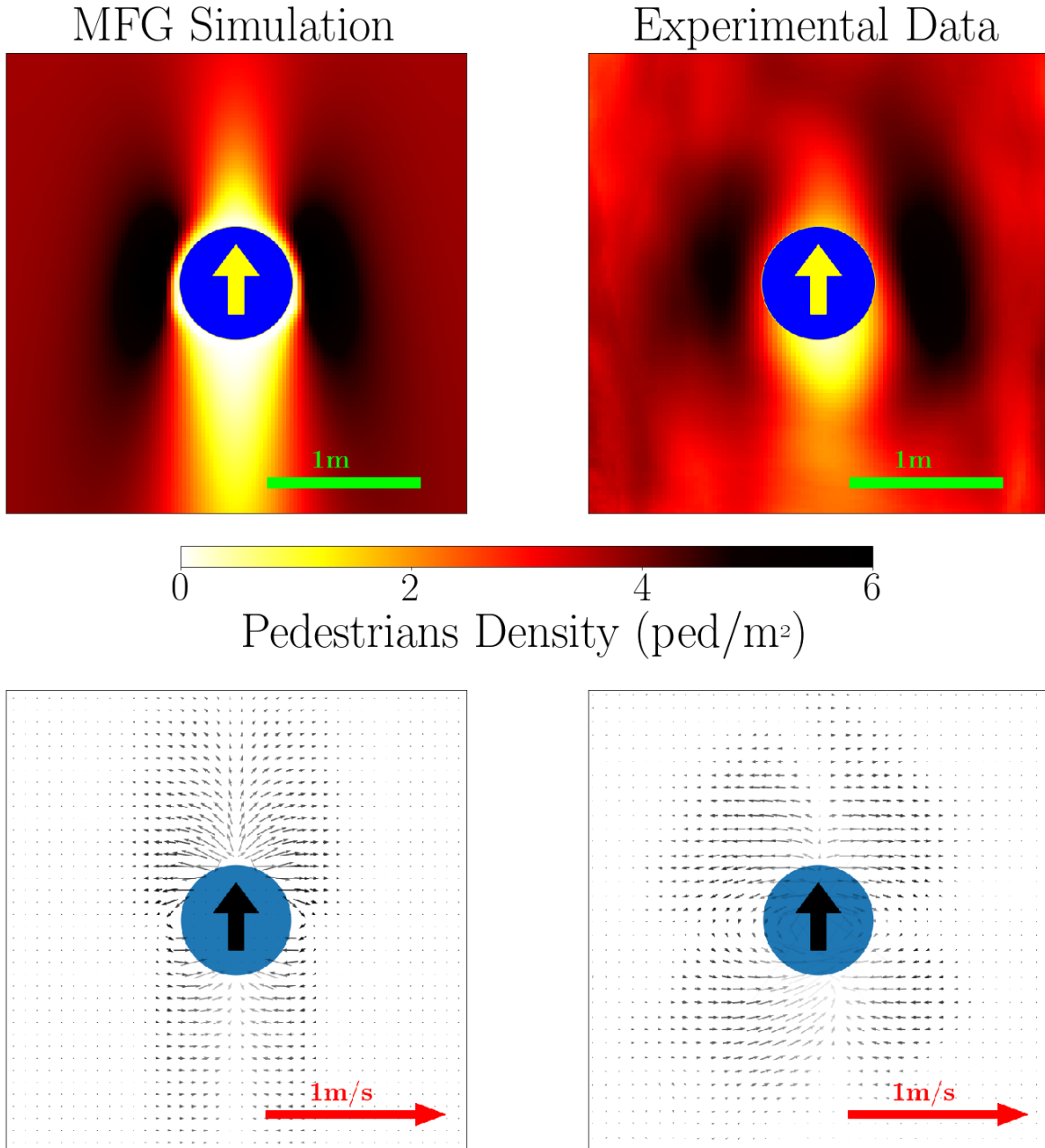


Figure 3: Qualitative comparison between density, first row, and velocity plots, second row, between the experiment, right column, and the ergodic state of the MFG model, with parameters $\xi = 0.2$, $c_s = 0.1$ and $\gamma = 0.5$, left column, for the case where pedestrians were oriented randomly.

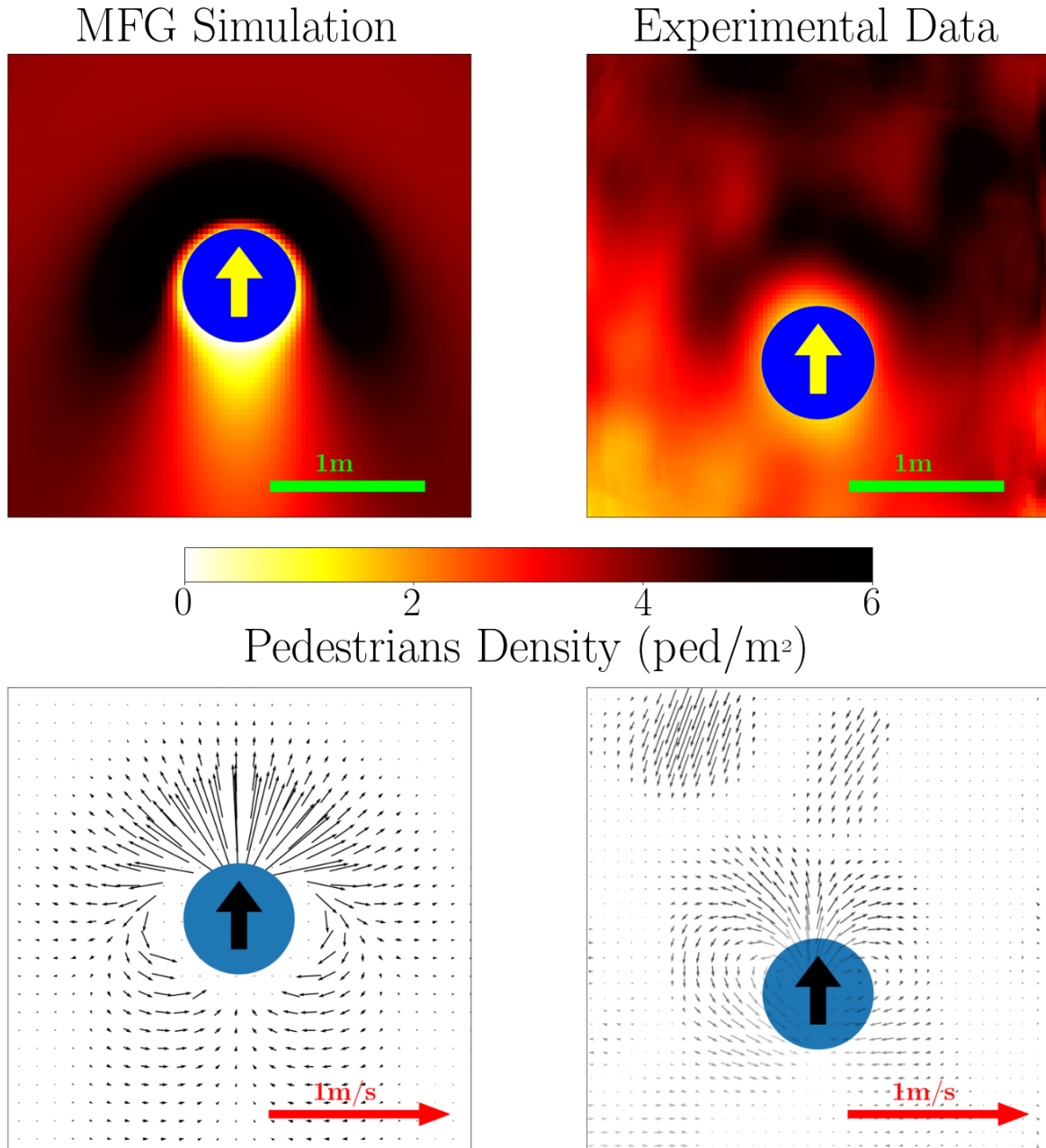


Figure 4: Qualitative comparison between density, first row, and velocity plots, second row, between the experiment, right column, and the ergodic state of the MFG model, with parameters $\xi = 0.4$, $c_s = 0.2$ and $\gamma = 6$, left column, for the case where pedestrians were giving their back to the incoming cylinder and were asked not to anticipate.

Acknowledgements

We acknowledge the precious help of Alexandre Nicolas who prepared and provided the experimental data used in this Paper. We acknowledge the careful reading of the manuscript by Alberto Rosso.

A Alternative formulation of MFG

In [7], we took advantage of the fact that by applying the Cole-Hopf transformation

$$u(\vec{x}, t) = -\mu\sigma^2 \log \Phi(\vec{x}, t), \quad (21)$$

one can cast the MFG equation in a form more familiar to physicists. In fact substituting (21) into equation (8) we obtain

$$\mu\sigma^2 \partial_t \Phi = -\frac{\mu\sigma^4}{2} \Delta \Phi - V[m]\Phi + \gamma\mu\sigma^2 \Phi \log \Phi. \quad (22)$$

The second part of this transformation amounts to defining $\Gamma(\vec{x}, t) = \frac{m(\vec{x}, t)}{\Phi(\vec{x}, t)}$ which, when plugged inside the KFP equation (9) yields

$$\mu\sigma^2 \partial_t \Gamma = \frac{\mu\sigma^4}{2} \Delta \Gamma + V[m]\Gamma - \gamma\mu\sigma^2 \Gamma \log m + \gamma\mu\sigma^2 \Gamma \log \Gamma. \quad (23)$$

Now, if $\gamma = 0$, we see that these equations have actually the same form of Non-linear Schrödinger equations, and this, as also explained in [17], enables the application of many of the tools developed in the NLSE field to MFG. Moreover, always for $\gamma = 0$, as explained in [7], casting the problem in this form is beneficial to the development of efficient numerical schemes, especially for the stationary state of MFG. Unfortunately the presence of the logarithmic term does pose significant problems for the numerical implementation when $\gamma > 0$. We nevertheless include the equations of the stationary state for completeness.

$$\lambda \Phi^e = -\frac{\mu\sigma^4}{2} \Delta \Phi^e - V[m^e]\Phi^e + \gamma\mu\sigma^2 \Phi^e \log \Phi^e, \quad (24)$$

$$-\lambda \Gamma^e = \frac{\mu\sigma^4}{2} \Delta \Gamma^e + V[m^e]\Gamma^e - \gamma\mu\sigma^2 \Gamma^e \log \Phi^e \Gamma^e + \gamma\mu\sigma^2 \Gamma^e \log \Gamma^e. \quad (25)$$

When passing to the moving frame, as in 2.3, the time dependent MFG in the Cole-Hopf settings become

$$\mu\sigma^2 \partial_t \check{\Phi} - \mu\sigma^2 \vec{s} \cdot \vec{\nabla} \check{\Phi} = -\frac{\mu\sigma^4}{2} \Delta \check{\Phi} - V[m]\check{\Phi} + \gamma\mu\sigma^2 \check{\Phi} \log \check{\Phi}, \quad (26)$$

$$\mu\sigma^2 \partial_t \check{\Gamma} - \mu\sigma^2 \vec{s} \cdot \vec{\nabla} \check{\Gamma} = \frac{\mu\sigma^4}{2} \Delta \check{\Gamma} + V[m]\check{\Gamma} - \gamma\mu\sigma^2 \check{\Gamma} \log m + \gamma\mu\sigma^2 \check{\Gamma} \log \check{\Gamma}, \quad (27)$$

whereas from (24) and (25) we get the corresponding equations for the stationary state

$$\lambda \check{\Phi}^e - \mu\sigma^2 \vec{s} \cdot \vec{\nabla} \check{\Phi}^e = -\frac{\mu\sigma^4}{2} \Delta \check{\Phi}^e - V[m_0]\check{\Phi}^e + \gamma\mu\sigma^2 \check{\Phi}^e \log \check{\Phi}^e, \quad (28)$$

$$-\lambda \check{\Gamma}^e - \mu\sigma^2 \vec{s} \cdot \vec{\nabla} \check{\Gamma}^e = \frac{\mu\sigma^4}{2} \Delta \check{\Gamma}^e + V[m_0]\check{\Gamma}^e - \gamma\mu\sigma^2 \check{\Gamma}^e \log m + \gamma\mu\sigma^2 \check{\Gamma}^e \log \check{\Gamma}^e. \quad (29)$$

B Details on the ergodic problem

Boundary conditions of the ergodic solution and the value of λ The motivation of this Appendix stems from the numerical implementation of the ergodic problem cast in the NLSE formalism, and in particular of the equations (28) and (27) for $\gamma = 0$, as in [7]. In this case, if one wishes to solve these time independent equations, the knowledge of boundary conditions is needed. To find these we look at what happens far from the obstacle, i.e. the asymptotic limits. In fact, we recall that in the experimental configuration, far from the intruder people were recorded not moving, meaning that, in the laboratory frame, they had null velocity. Therefore, when passing to the moving frame, agents at the boundary should move with velocity $-\vec{s}$ and the density should be constant equal to the average value m_0 . We can derive the velocity of an agent at time t and position \vec{x} from (18), in fact we have that

$$\begin{aligned}\partial_t \tilde{m} &= \frac{\sigma^2}{2} \Delta \tilde{m} + \vec{s} \cdot \nabla \tilde{m} + \frac{1}{\mu} \nabla \cdot (\tilde{m} \nabla \tilde{u}) \\ &= \nabla \cdot \left(\frac{\sigma^2}{2} \nabla \tilde{m} + \vec{s} \tilde{m} + \frac{1}{\mu} (\tilde{m} \nabla u) \right) \\ &= -\nabla \cdot \vec{j}\end{aligned}\quad (30)$$

Therefore, being $\vec{j} = \tilde{m} \vec{v}$, the velocity is given by

$$\vec{v} = -\frac{\nabla \tilde{u}}{\mu} - \vec{s} - \frac{\sigma^2 \nabla \tilde{m}}{2\tilde{m}}, \quad (31)$$

and the same is done for the ergodic state. Far from the perturbation caused by the cylinder, the fact that the density is supposed constant means $\nabla \tilde{m}_{asy}^e \simeq \vec{0}$, and the fact that people move with velocity $-\vec{s}$ means $\vec{v}_{asy}^e = -\vec{s}$. Finally we obtain $\nabla \tilde{u}_{asy}^e = 0$ and $\nabla \tilde{\Phi}_{asy}^e = 0$, leaving us with $\tilde{\Phi}_{asy}^e = C(t)$. In order to fix $C(t)$ we recall that $\tilde{\Phi}_{asy}^e \tilde{\Gamma}_{asy}^e = m_0$, meaning that one can take $C(t) \equiv \sqrt{m_0}$. Substituting the asymptotic solution in either (28) or (29) one obtains

$$\lambda = -g m_0 + \gamma \mu \sigma^2 \log \sqrt{m_0}. \quad (32)$$

Gauge invariance of the $\gamma = 0$ case It is worth mentioning an interesting properties of equation (19) when $\gamma = 0$. Let us consider the substitution $\tilde{u} = \bar{u} - \mu \vec{v} \cdot \vec{r}$, with \vec{v} generic velocity. When put into (19) with $\gamma = 0$ we obtain the equation

$$\tilde{V}[\tilde{m}] = \frac{\sigma^2}{2} \Delta \bar{u} - \frac{1}{2\mu} (\vec{\nabla} \bar{u})^2 - \bar{\lambda} - (\vec{s} - \vec{v}) \cdot \vec{\nabla} \bar{u} + \mu \vec{v} \cdot \left(\vec{s} - \frac{\vec{v}}{2} \right) \quad (33)$$

Applying the same substitution to the definition of the velocity (31) gives

$$\vec{v} = -\frac{\nabla \bar{u}}{\mu} - (\vec{s} - \vec{v}) - \frac{\sigma^2 \nabla \tilde{m}}{2\tilde{m}}, \quad (34)$$

that, considering the asymptotic behavior, when put equal to $-\vec{s}$ gives, $\nabla \bar{u}_{asy} = \mu \vec{v}$. The first thing we observe is that putting this into (33) the equation for the asymptotic behavior is

$$\nabla \tilde{\Phi}_{asy}^e = -\frac{\mu \gamma}{\sigma^2} \tilde{\Phi}_{asy}^e,$$

that, when solved gives

$$\bar{\Phi}_{asy}^e = \sqrt{m_0} e^{-\frac{\mu \vec{v} \cdot \vec{r}}{\sigma^2}}, \quad \bar{\Gamma}_{asy}^e = \sqrt{m_0} e^{\frac{\mu \vec{v} \cdot \vec{r}}{\sigma^2}} \quad (35)$$

that, in the Schrödinger representation, can be seen as a Gauge transformation.

C Details on the numerics

In this section we want to explain the details of the simulations of Figures 2, 3, and 4. These pictures represent the ergodic state of the MFG problem. To obtain them we have solved the time dependent equations (8) and (9) by using the ode45 MATLAB routine on a rectangular grid of 400×560 points, with $dx = dy = 0.025$. The equations are coupled, HJB is solved backward and KFP is solved forward. Therefore, what we do is, we first solve backward u starting from a final condition equal to 0 everywhere, with m fixed and equal to $m_0 = 3.5ped/m^2$. We simulate the moving cylinder by taking U_0 to be equal to a large negative value in a circle of radius $R = 0.37m$ and with center moving from $-5m$ to $5m$ in the vertical direction, with speed $0.6m/s$. Once the solution for u has been computed for all times from T to t_0 , with time-step $dt = 0.14$, we solve KFP to obtain m , that we use to solve again u and then again m , until the mean squared error between two consecutive solutions of m is smaller than 10^3 . We have chosen the dimensions of the simulated area large enough to have the cylinder completely surrounded for most of the simulation time T , chosen so that the intruder can complete its journey, and we can therefore access the ergodic state of the system for $t = T/2$, which is what is showed in Figures 2, 3, and 4.

References

- [1] S. P. Hoogendoorn and P. H. Bovy, *Pedestrian route-choice and activity scheduling theory and models*, Transportation Research Part B: Methodological **38**(2), 169 (2004), doi:[https://doi.org/10.1016/S0191-2615\(03\)00007-9](https://doi.org/10.1016/S0191-2615(03)00007-9).
- [2] D. Helbing and P. Molnar, *Social force model for pedestrian dynamics*, Physical review E **51**(5), 4282 (1995), doi:<https://doi.org/10.1103/physreve.51.4282>.
- [3] F. Zanlungo, T. Ikeda and T. Kanda, *Social force model with explicit collision prediction*, EPL (Europhysics Letters) **93**(6), 68005 (2011), doi:[10.1209/0295-5075/93/68005](https://doi.org/10.1209/0295-5075/93/68005).
- [4] I. Karamouzas, B. Skinner and S. J. Guy, *Universal power law governing pedestrian interactions*, Physical review letters **113**(23), 238701 (2014), doi:<https://doi.org/10.1103/PhysRevLett.113.238701>.
- [5] I. Echeverría-Huarte and A. Nicolas, *Anticipating collisions, navigating in complex environments, elbowing, pushing, and smartphone-walking: A versatile agent-based model for pedestrian dynamics*, doi:[10.48550/ARXIV.2211.03419](https://doi.org/10.48550/ARXIV.2211.03419) (2022).
- [6] A. Nicolas, M. Kuperman, S. Ibañez, S. Bouzat and C. Appert-Rolland, *Mechanical response of dense pedestrian crowds to the crossing of intruders*, Scientific Reports **9**(105) (2019), doi:<https://doi.org/10.1038/s41598-018-36711-7>.

- [7] T. Bonnemain, M. Butano, T. Bonnet, I. Echeverría-Huarte, A. Seguin, A. Nicolas, C. Appert-Rolland and D. Ullmo, *Pedestrians in static crowds are not grains, but game players*, doi:[10.48550/ARXIV.2201.08592](https://doi.org/10.48550/ARXIV.2201.08592) (2022).
- [8] J.-M. Lasry and P.-L. Lions, *Jeux à champ moyen. i – le cas stationnaire*, C. R. Acad. Sci. Paris **343**(9), 619 (2006), doi:<https://doi.org/10.1016/j.crma.2006.09.019>.
- [9] J.-M. Lasry and P.-L. Lions, *Jeux à champ moyen. ii – horizon fini et contrôle optimal.*, C. R. Acad. Sci. Paris **343**(10), 679 (2006), doi:<https://doi.org/10.1016/j.crma.2006.09.018>.
- [10] M. Huang, R. P. Malhamé and P. E. Caines, *Large population stochastic dynamic games: closed-loop McKean–Vlasov systems and the nash certainty equivalence principle*, Commun. Inf. Syst. **6**(3), 221–252 (2006), doi:<https://doi.org/cis/1183728987>.
- [11] P. Cardaliaguet, *Notes on mean field games*, <https://www.ceremade.dauphine.fr/~cardaliaguet/MFG20130420.pdf> (2012).
- [12] D. A. Gomes and J. Saúde, *Mean field games models – a brief survey.*, J. Dyn. Games Appl. **4**(2), 110 (2014), doi:<https://doi.org/10.1007/s13235-013-0099-2>.
- [13] A. Bensoussan, J. Frehse and S. C. P. Yam, *The master equation in mean field theory.*, J. Math. Pures Appl. **103**(6), 1441–1474 (2015), doi:<https://doi.org/10.1016/j.matpur.2014.11.005>.
- [14] P. Cardaliaguet, F. Delarue, J.-M. Lasry and P.-L. Lions, *The Master Equation and the Convergence Problem in Mean Field Games*, Princeton University Press, doi:<https://doi.org/10.23943/princeton/9780691190716.001.0001> (2019).
- [15] R. Carmona and F. Delarue, *Probabilistic analysis of mean-field games.*, SIAM J. Control Optim. **51**(4), 2705 (2013), doi:<https://doi.org/10.1137/120883499>.
- [16] A. Lachapelle and M.-T. Wolfram., *On a mean field game approach modeling congestion and aversion in pedestrian crowds.*, Transportation Research Part B **45**(10), 1572–1589 (2011), doi:<https://doi.org/10.1016/j.trb.2011.07.011>.
- [17] D. Ullmo, I. Swiecicki and T. Gobron, *Quadratic mean field games*, Physics Reports **799**, 1 (2019), doi:<https://doi.org/10.1016/j.physrep.2019.01.001>.
- [18] R. Bellman, R. Bellman and R. Corporation, *Dynamic Programming*, Princeton University Press, doi:<https://doi.org/10.1515/9781400835386> (1957).
- [19] P. Cardaliaguet, J.-M. Lasry, P.-L. Lions and A. Porretta, *Long time average of mean field games with a nonlocal coupling*, SIAM J. Control Optim **51**(5), 3558 (2013), doi:<https://doi.org/10.1137/120904184>.